Molecular Influences on the Quantification of Lewis Acidity with Phosphine Oxide Probes

*Riddhi R. Golwankar,[a,‡] T. Davis Curry II,[a,‡] Cecilia J. Paranjothi,[a] and James D. Blakemore[a,]**

[a] Department of Chemistry, University of Kansas,

1845 Irving Hill Road, Lawrence, Kansas 66045 United States

‡ These authors contributed equally.

* To whom correspondence should be addressed. E-mail: blakemore@ku.edu

KEYWORDS: Titrations; NMR spectroscopy; metal salts; organic solvent; acidity.

ABSTRACT: Gutmann-Beckett-type measurements with phosphine oxide probes can be used to estimate effective Lewis acidity with ^{31}P nuclear magnetic resonance spectroscopy, but the influence of the molecular structure of a given probe on the quantification of Lewis acidity remains poorly documented in experimental work. Here, a quantitative comparison of triethyl (**E**), trioctyl (**O**), and triphenyl (**P**) phosphine oxides as molecular probes of Lewis acidity has been carried out via titration studies in MeCN with a test set of six mono- and di-valent metal triflate salts. In comparison to **E**, the bulkier **O** displays a similar range of chemical shift values and binding affinities for the various test metal ions. Spectral linewidths and speciation properties vary for

individual cation-to-probe ratios, however, confirming probe-specific properties that can impact data quality. Importantly, **P** displays a consistently narrower dynamic range than both **E** and **O**, illustrating how electronic changes at phosphorus can influence NMR response. Comparative parametrizations of the effective Lewis acidities of a broader range of metal ions, including the trivalent rare earth ions Y^{3+}, Lu^{3+}, and Sc^{3+} as well as the uranyl ion (UO_2^{2+}), can be understood in light of these results, informing on the fundamental chemical processes underlying the useful approach of single-point measurements for quantification of effective Lewis acidity. Together with a study of counter-anion effects reported here, these data clarify the diverse ensemble of factors that can influence the measurement of Lewis acid:base interactions.

INTRODUCTION

Addition or incorporation of Lewis acidic metal cations into redox-active metal complexes has emerged as an attractive strategy for promoting new reactivity patterns and enabling otherwise inaccessible transformations.[1] Understanding the role(s) of the Lewis acids in such systems is a topic of particular importance, because the mechanisms underlying the observed reactivity could be modulated by the Lewis acids in a variety of ways. Among these, tuning of reduction potentials is of particular interest in small-molecule activation and redox processing of metal complexes, aspects that could impact applications in energy science and sustainability.[2,3]

Work across a number of fields has demonstrated that electropositive metal ions can effectively function as Lewis acids for modulating redox reactivity. Metal ions that are commonly used for these purposes span a wide range of sizes and coordination numbers, and often include mono-, di-, and trivalent ions such as Na^+, Ca^{2+}, and Y^{3+}.[4] Strongly Lewis acidic trivalent cations such as Sc^{3+} attract special attention, as the effects they promote are typically more pronounced than those

engendered by more weakly acidic mono- and di-valent cations.[5] Understanding the different effects engendered by various metal ions, however, could allow the effects to be controlled and used for rational design of new chemistries.

In this regard, the quantification of effective Lewis acidity remains an area of significant ongoing work, despite the initiation of such efforts decades ago.[6,7] The Gutmann-Beckett method is perhaps best known, an approach in which Lewis acidity is interrogated with ^{31}P nuclear magnetic resonance (NMR) spectroscopy and a suitable phosphorus-containing probe molecule, typically a phosphine oxide.[8] Recently, we reported uniform measurements of the Lewis acidities of a family of mono-, di-, and tri-valent redox inactive metal ions (in the form of their triflate salts) in both d_3-MeCN and CD_2Cl_2, polar organic solvents commonly used for mechanistic studies of redox chemistry.[9] Our comprehensive measurements complemented prior work that had focused on individual metal ions and some transition metal complexes,[10] and they highlighted that association constants and concentration-dependent equilibria can be measured through titration studies and should be considered in studies of Lewis-acid modulated chemistry.

However, we were surprised to find that less attention has been paid to experimental comparison of the properties of different phosphine oxide probe molecules within the framework of the Gutmann-Beckett method. For example, in our prior work, we utilized triphenylphosphine oxide (**P**) as the probe molecule in consideration of its high chemical stability and low cost (less than $1 per gram).[9] However, the consequences of substituting one probe for another are not well documented, leading to ambiguities that could preclude design of improved assays for Lewis acidity. Work has compared the spectral changes associated with formation of various Lewis acid-base pairs,[11] and some focus has been placed on explanation of the NMR properties of various phosphine oxides.[12] But, to the best of our knowledge, no systematic comparisons of the titration

behavior of even a limited set of phosphine oxide probe molecules are available. We anticipated that experimental comparison of phosphine oxide probes could provide insights into the specific features of the probes that govern the experimental observables affording quantitative measurements of effective Lewis acidity.

Here, we report comparison of triethyl- (**E**), trioctyl- (**O**), and triphenyl- (**P**) phosphine oxides as molecular probes of effective Lewis acidity, using triflate salts of mono-, di-, and trivalent cations as a testbed for comparison of the probes. Titration data collected by $^{31}P\{^{1}H\}$ NMR in MeCN reveal that all three probes bind to Na^+ and K^+ with 1:1 stoichiometry,[13] whereas they bind to Li^+, Ba^{2+}, Sr^{2+}, and Ca^{2+} with greater than 1:1 stoichiometry as shown by data fitting to the Hill-Langmuir equation (HLE) and determination of the Hill coefficient as a measure of cooperativity.[14] In this context, cooperativity indicates greater than 1:1 binding stoichiometry; apparent interaction energies (estimated from linearized titration data) can be interpreted as a function of both *i*) the identity of the probe molecule and *ii*) the effective Lewis acidity of the cation being studied. In both the titrations and single-point measurements, **E** and **O** display a significantly larger dynamic range than **P**, suggesting a greater intrinsic ability to distinguish similar chemical species. However, spectral linewidths in individual experiments at specific cation-to-probe ratios can vary between probes, confirming a less sensitive probe such as **P** may be preferred in a specific context. Taken together, the findings of this study expand the experimental toolkit for quantification of Lewis acidity with phosphine oxide probes.

RESULTS

Preparation of Metal Cations and Probes

In this work, we selected triflate (OTf^-) salts as the testbed for comparison of the phosphine oxide probe molecules. In particular, we selected common monovalent cations (Cs^+, Rb^+, K^+, Na^+, and Li^+) and divalent cations (Ba^{2+}, Sr^{2+}, Ca^{2+}, and Zn^{2+}) as well as a few more challenging trivalent cations (Y^{3+}, Lu^{3+}, and Sc^{3+}) and uranyl triflate ($UO_2(OTf)_2$). We included uranyl triflate in our study because of *i)* its unique solubility in MeCN,[15] *ii)* its relevance to studies of uranium redox chemistry, and *iii)* the recognized highly Lewis acidic nature of uranyl in water.[4] The Lewis acidity of the uranyl ion has not previously been measured in MeCN, to the best of our knowledge, and uranyl triflate is ideal for this purpose.

KOTf, NaOTf, LiOTf, $Ba(OTf)_2$, $Ca(OTf)_2$, $Zn(OTf)_2$, $Y(OTf)_3$, $Lu(OTf)_3$, and $Sc(OTf)_3$ are commercially available, and were confirmed to be anhydrous after extensive drying (180ºC for 24 h; see Experimental Section) by infrared (IR) spectroscopy (see Supporting Information, Figures S10-S20). We also previously collected ^1H and ^{19}F NMR spectra of these salts, which showed no organic or solvent impurities.[9] The IR spectra reported in this work strongly resemble those of the same materials reported in our prior work, confirming the appropriateness of the dried compounds for work here. RbOTf, CsOTf, $Sr(OTf)_2$, and $UO_2(OTf)_2$ are not commercially available; the former three were prepared according to procedures described in our previous work[9] while $UO_2(OTf)_2$ was prepared according to the procedure from Ephritikhine and co-workers (see Experimental Section for details).[16] Following extensive drying similar to the commercial salts (180ºC for 24 h), characterization by IR spectroscopy (see Supporting Information, Figures S8, S9, S17, and S21) confirmed the purity of these synthesized materials; we also collected ^1H and ^{19}F NMR spectra for the newly generated $UO_2(OTf)_2$ material (see SI, Figures S22 and S23).

In order to compare probe molecules, we selected triethyl (**E**), trioctyl (**O**), and triphenyl (**P**) phosphine oxides for study. All three of these compounds are commercially available from a wide variety of suppliers, motivating their use as probes. In particular, **O** was investigated on the basis of its low cost ($2 per gram **O** vs. $66 per gram **E**) as well as the analogous nature of its octyl groups to the more compact ethyl groups in more commonly investigated **E**. Each probe (see Experimental Section) was found to be stable under ambient conditions and was dried *in vacuo* (30ºC for 24 h) upon receipt from the commercial supplier. On the basis of IR as well as ^{1}H and ^{31}P NMR spectroscopies, the probes were confirmed clean, dry, and ready for testing (see SI, Figures S1-S7 and S90).

Methodological Considerations for Use of Non-Deuterated Solvent

At the outset of this investigation, we surmised that a large number of titrations and individual NMR experiments would be required, a prospect associated with significant consumption of deuterated solvent and thus high cost ($3.00 per gram d_3-MeCN vs. $0.10 per gram MeCN). In our prior work, we focused on a single probe molecule (**P**) and thus the costs were more manageable for work in d_3-MeCN. Working in d_3-MeCN has the advantage that no sample of an internal or external standard is needed for calibration of the ^{31}P-NMR probe signal; the established and recommended scale using a ratio of absolute frequencies (Ξ; a virtual external standard) was used to report data relative to H_3PO_4.[17]

In the work reported here, the "solvent burden" was further exacerbated by the need to maintain constant probe molecule concentration across the range of varying cation concentrations.[13] For each experiment, a unique sample must be prepared, corresponding to the specific cation-to-probe ratio being interrogated. This requirement has been discussed with great clarity in the work of

Thordarson,[13] in the context of the field of supramolecular chemistry, particularly; strict maintenance of constant probe concentration across experiments was used here in order to enable rigorous comparisons between the probe molecules. In fact, we found the measurements of Lewis acidity reported in this work to be sensitive to changes in the concentration of the probe molecule (see SI, Figures S30-S34 and Table S1). This observation prompted thorough characterization of the solvents used for experiments, including the quantification of adventitious water in our dried MeCN (see Experimental Section). Water could act as a competing ligand to metal cations and/or hydrogen bond to the probes, so confirming the dryness of samples was paramount to ensuring the reliability of our measurements. We determined that the concentration of water in our MeCN was less than 1% of the concentration of probe molecule used in our standardized measurements (37 μM H_2O vs. 10 mM probe; see SI, Figure S37 and Tables S3 and S4), suggesting the effect of trace water on our measurements would be minimal.

Thus, motivated by the enduring utility of MeCN as a polar aprotic solvent, we employed a method for carrying out titrations in dry, non-deuterated MeCN by $^{31}P\{^{1}H\}$ NMR spectroscopy. In order to do this, capillary tubes were prepared containing 0.1 M tetrabutylammonium hexafluorophosphate (TBAP) as an external ^{31}P NMR standard in MeCN. Titration experiments could thus be carried out in MeCN referenced to the external standard of TBAP. The signal for TBAP was referenced to H_3PO_4 (as recommended by IUPAC[17]) through use of the standard tabulated ratios of heteronuclear resonant frequencies (Ξ values) in a single, separate experiment carried out in d_3-MeCN; a series of control experiments demonstrated that both the chemical shift of TBAP in MeCN within a capillary tube and the chemical shift of **E** referenced to the external standard of TBAP are both consistent with their respective measurements in d_3-MeCN (see SI, Figures S24 and S25). Titration of **E** with NaOTf was carried out in both d_3-MeCN and MeCN

and the results were found to be virtually identical (see SI, Figures S26-S29), providing further evidence that our approach used here is up to the task.

Comparison of Full Titrations with Monovalent Cations

As the starting point for comparisons between the probe molecules, we initially compared the behavior of **E**, **O**, and **P** when titrated with the monovalent ions K^+ and Na^+ (see Figure 1). In this effort, the ^{31}P chemical shift ($\delta^{31}P$) was measured for 10 mM samples of probe in the presence of increasing concentrations of the cation of interest. As anticipated on the basis of our prior work,[9] the change in chemical shift ($\Delta\delta^{31}P$) increased as the cation concentration was increased, initially undergoing a greater change but eventually leveling off at higher titrant cation equivalencies. Inspection of the raw $^{31}P\{^1H\}$ NMR data (see Supporting Information, Figures S39-S50) shows that the smaller Na^+ ion results in the larger absolute shifts in $\Delta\delta^{31}P$, as expected on the basis of anticipated charge density about the metal center.

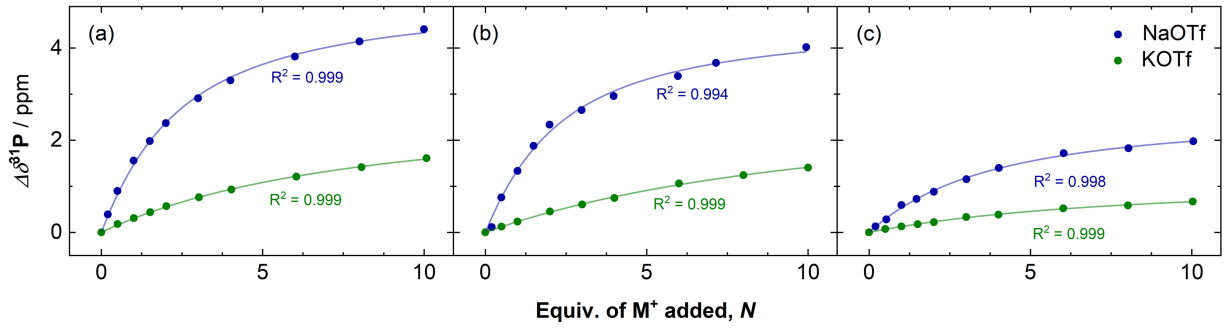

Figure 1. Titration of **E** (panel a, left), **O** (panel b, middle), and **P** (panel c, right) with NaOTf (blue points) and KOTf (green points). Fits to the 1:1 binding isotherm are given in the blue and green lines, respectively. For clarity, data points for larger additions of KOTf were omitted from this image to harmonize the appearance of the plots; full datasets for titrations with KOTf are shown in SI, Figures S63 and S64.

To extract the parameters that quantify binding affinity and effective Lewis acidity, we first fitted the titration data for Na^+ and K^+ to the 1:1 binding isotherm equation, which has the form given below in equation 1.[9,13]

$$\frac{\Delta\delta}{\Delta\delta_{max}} = \frac{1}{2}\left[\left(1 + N + \frac{1}{K_a[H_0]}\right) - \sqrt{\left(1 + N + \frac{1}{K_a[H_0]}\right)^2 - 4N}\right] \qquad (1)$$

In this expression, $\Delta\delta$ is the observed change in chemical shift of the ^{31}P-containing probe, N is the number of equivalents of metal ion added with respect to probe, K_a is the calculated association constant for probe-cation binding, $\Delta\delta_{max}$ is the calculated change in chemical shift of the probe at infinite excess of metal cation, and $[H_0]$ is the concentration of probe molecule (10 mM across all experiments unless otherwise noted). The 1:1 binding isotherm is derived from the assumption that only a single equilibrium for probe-cation binding is operative; in other words, one metal cation can coordinate to a single probe molecule. Both *i*) the agreement of the shape of the fitted curves

with the overall profile of the experimental data and *ii*) the quantified goodness-of-fit values (R^2 values, see Figure 1) support the 1:1 binding stoichiometry for these cations to **E**, **O**, and **P**.

Similar to findings in our prior work, the fitted $\Delta\delta_{max}$ values are greater for Na^+ than for K^+ in the cases of all three probes (see Table 1). As judged by the pK_a values of their aqua complexes in water,[4] Na^+ is a stronger Lewis acid in water than K^+. As indicated by the measured K_a values, Na^+ also binds more tightly to each probe in MeCN than K^+ does, consistent with the notion that smaller, more charge-dense ions may bind preferentially to phosphine oxides in MeCN.

Table 1. Fitted parameters with the 1:1 binding isotherm for the titrations with NaOTf and KOTf.

Parameter	Probe	NaOTf [b]	KOTf [b,c]
pK_a of $[\mathbf{M}(H_2O)_m]^+$ [a]	-	14.8	16.0
K_a (M^{-1})	**E**	54.84 ± 2.97	12.60 ± 0.44
	O	57.47 ± 6.65	7.05 ± 0.46
	P	31.22 ± 2.14	14.46 ± 0.75
$\Delta\delta_{max}$ ^{31}P (ppm)	**E**	5.19 ± 0.09	2.95 ± 0.05
	O	4.67 ± 0.16	3.53 ± 0.12
	P	2.66 ± 0.07	1.14 ± 0.03

[a] Measured in water and taken from ref. 4. [b] Errors were calculated from the direct nonlinear fit of eq. 1 and are given as ±1σ. [c] Fitted parameters for titrations with KOTf are from full datasets shown in Figures S63 and S64.

When comparing the probes, **E** and **O** are strikingly similar. The similar K_a values for both these monovalent ions suggest that steric bulk provided by the octyl chains of **O** does not hinder the binding of a single cation to the probe when compared to the smaller ethyl groups. The similarity in the $\Delta\delta_{max}$ values between **E** and **O** for both cations points to a similar ability of the probes to distinguish different metal cations. On the other hand, **P** has a markedly smaller dynamic range in

studies of these ions than **E** and **O**. Indeed, for mild Lewis acids like Na^+ and K^+, the changes in chemical shift of **P** at small additions of metal cation were quite minor (for example, $\Delta\delta$ is only 0.08 ppm upon addition of 0.5 eq. of K^+ to **P**), and the $\Delta\delta_{max}$ values for **P** are consistently smaller (less than half) than those of **E** and **O**. **P** could be thought to bind more weakly than the other probes, but, interestingly, the approach of quantitative titration deconvolutes the chemical equilibrium differences. Consequently, the difference in dynamic range can be concluded to *not* have its origin in the chemical equilibrium of probe binding, but rather in the intrinsic nature of **P** vs. **E** and **O**.

Comparison of Full Titrations with Divalent Cations and Li^+

Next, we sought to compare the behavior of **E**, **O**, and **P** with metal cations that could be anticipated to be effectively stronger Lewis acids. From our previous work,[9] we expected that divalent cations would serve here as stronger Lewis acids than monovalent ions and that they would deviate from 1:1 binding, at least in the case of **P** as probe, making the 1:1 binding isotherm a poor fitting function for titrations of **P** with divalent ions. Here, we carried out full titrations of three divalent ions, Ba^{2+}, Sr^{2+}, and Ca^{2+}, with **E**, **O**, and **P**. Perhaps due to its small size, Li^+ behaves similarly to the divalent metal cations in terms of its displayed binding stoichiometry and relatively high Lewis acidity; here, we discuss titrations with Li^+ together with the divalent ions. In line with our prior report,[9] we used the Hill-Langmuir equation (HLE) in this effort; this equation is perhaps most famous for enabling quantitative study of O_2 binding to hemoglobin, as it can effectively describe multi-equilibrium effects,[14] and has the form given in equation 2.

$$\Delta\delta = \frac{\Delta\delta'_{\max}(N)^{\alpha}}{(K_{1/2})^{\alpha}+(N)^{\alpha}} \quad (2)$$

The HLE is especially useful for modeling systems where multiple equilibria are operative in determining solution speciation.[14] In this expression, $\Delta\delta$ is the observed change in ^{31}P chemical shift of the probe, N is the number of equivalents of metal cation added with respect to the probe, $\Delta\delta'_{max}$ is the calculated change in chemical shift of the probe at infinite excess of metal cation, $K_{1/2}$ is the number of equivalents required to change the chemical shift of the probe by one half of $\Delta\delta'_{max}$, and α is the so-called Hill coefficient.[14] The Hill coefficient is perhaps the most distinctive feature of the HLE, allowing this expression to be quite versatile in modeling situations where multiple equilibria occur and interact. In work of the type reported here, one can imagine multiple probe molecules binding to a single cation, or multiple cations binding to one probe. An α value greater than one, classically referred to as "positive cooperativity," can be interpreted in our system as the presence of equilibria wherein multiple metal ions can bind to one probe.[9] In our work discussed here, systems with positive cooperativity give titration data with a sigmoidal shape. With increasing amounts of added metal cation, the statistical likelihood increases of binding multiple metal ions to a single probe molecule; the change in chemical shift of the probe increases disproportionately at larger additions of metal cation as compared to simple 1:1 binding, up to a final maximum value at which point the change in chemical shift becomes negligible.

In the series of divalent ions tested, the $\Delta\delta'_{max}$ values increase as the charge density of the cations increases for all three probes (see Figure 2). This can also be viewed for the divalent ions in terms of decreasing ionic radius, which drives increasing charge density. Li^+ displays systematically higher $\Delta\delta'_{max}$ values than Ba^{2+}, suggesting that charge is not the only determinant of $\Delta\delta'_{max}$, however, and highlighting the utility of charge density in making comparisons between valencies.

On the other hand, Li^+ has a much lower binding affinity for all three probes compared to the divalent ions, as indicated by the larger $K_{1/2}$ values for the titrations of **E**, **O**, and **P** with Li^+.

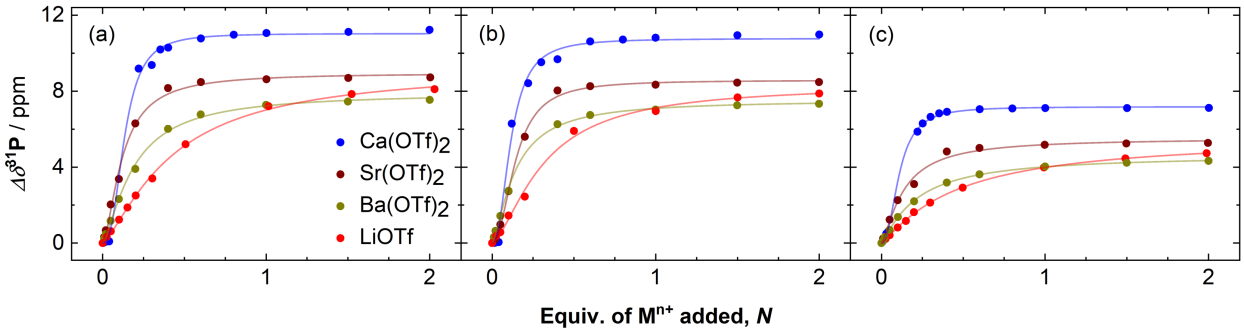

Figure 2. Titration of **E** (panel a, left), **O** (panel b, middle), and **P** (panel c, right) with $Ca(OTf)_2$ (blue points), $Sr(OTf)_2$ (burgundy points), $Ba(OTf)_2$ (yellow points) and LiOTf (red points). Fits to the HLE are given in light blue, light burgundy, light yellow, and light red, respectively.

Comparing the probes, **P** has a much smaller dynamic range than **E** and **O** as estimated in the data collected for the divalent ions, similar to the case of the monovalent ions (see Table 2 for quantified parameters). Generally speaking, the profile of the chemical shift vs. metal ion concentration data are very similar for **E** and **O** (*cf.* data in panels a and b in Figure 2). Nonetheless, **O** displays a slightly smaller dynamic range than **E**; the possible origin of these differences in chemical shift range is discussed later in this paper (*vide infra*), but we do note here that we anticipated at the outset of this study that the chemical shift tensors governing the ^{31}P-NMR properties of the probes[18] should be similar on the basis of similar atomic connectivity in all three cases. And, most clearly, there is a marked difference in the sensitivity to different chemical species between the trialkyl phosphine oxides and **P**. On the basis of the fitting to the HLE, **E** and **O** often display behavior that is more "positively cooperative" than **P**, as quantified by the greater value of

the Hill coefficient. This behavior could arise from multiple factors, from among which we will note here that the trialkyl phosphine oxides could be anticipated on the basis of inductive effects to be more electron rich; this could drive stronger association with the cations on the basis of their anticipated higher Lewis basicity. These factors are considered in detail in the Discussion Section.

Table 2. Parameters from Hill-Langmuir fit for titrations of the series of metal ions studied with all three probes.

Parameters	Probe	Guest					
		$Ca(OTf)_2$	**$Sr(OTf)_2$**	**$Ba(OTf)_2$**	**LiOTf**	**NaOTf**	**KOTf** [d]
pK_a of $[\mathbf{M}(H_2O)_m]^{n+}$ [a]	-	12.6	13.2	13.4	13.8	14.8	16.06
Ionic radius of **M** (Å) [b]	-	1.12	1.40	1.56	1.06	1.18	1.65
$\Delta\delta'_{max}$ ^{31}P (ppm) [c]	**E**	11.22 ± 0.14	8.95 ± 0.17	7.92 ± 0.14	8.79 ± 0.10	5.74 ± 0.08	3.40 ± 0.12
	O	10.77 ± 0.20	8.57 ± 0.09	7.53 ± 0.11	8.50 ± 0.15	4.62 ± 0.30	4.48 ± 0.45
	P	7.18 ± 0.04	5.52 ± 0.19	4.65 ± 0.04	5.53 ± 0.03	2.73 ± 0.19	1.09 ± 0.06
$K_{1/2}$ (equiv.) [c]	**E**	0.14 ± 0.01	0.12 ± 0.01	0.19 ± 0.01	0.39 ± 0.01	2.91 ± 0.10	11.45 ± 0.88
	O	0.11 ± 0.01	0.14 ± 0.01	0.14 ± 0.01	0.32 ± 0.02	2.18 ± 0.31	24.44 ± 5.33
	P	0.11 ± 0.01	0.14 ± 0.01	0.21 ± 0.01	0.44 ± 0.01	3.90 ± 0.60	6.77 ± 0.80
α [c]	**E**	2.47 ± 0.28	1.63 ± 0.13	1.40 ± 0.07	1.44 ± 0.05	0.95 ± 0.02	0.93 ± 0.02
	O	2.29 ± 0.28	2.13 ± 0.12	1.42 ± 0.07	1.46 ± 0.09	1.13 ± 0.11	0.88 ± 0.04
	P	2.29 ± 0.07	1.36 ± 0.16	1.19 ± 0.02	1.16 ± 0.02	1.04 ± 0.07	1.07 ± 0.05

[a] From reference 4. [b] From reference 19, assuming C.N. = VIII in all cases. [c] Errors were calculated from the direct nonlinear fit of eq. 2 and are given as ±1σ. [d] Fitted parameters for titrations with KOTf are from full datasets shown in Figures S63 and S64.

For titrations of **E**, **O**, and **P** with Na^+ and K^+, re-fitting of the titration data to the HLE in place of the 1:1 binding isotherm returns α values in all cases that are close to unity, re-confirming that binding of Na^+ and K^+ to **E**, **O**, and **P** follow a rigorous 1:1 stoichiometry (see Table 2, right two columns, as well as SI, Figure S63). These findings, along with the results of fitting the titration data for the divalent ions to the HLE, underscore the utility of the HLE as a broadly applicable function for unified quantification of titration data across systems displaying quite distinctive

solution-phase behaviors. As understanding the behavior of different classes of metal ions remains difficult, HLE-based approaches are attractive.

When rationalizing the influence of secondary metal cations on chemical systems of interest, trends have been discussed in the literature in terms of charge, ionic radius,[19] and various scales of effective Lewis acidity. Of these descriptors, effective Lewis acidity is perhaps the most ill-defined, generally speaking, since most quantifications of Lewis acidity depend on the identity of the formal Lewis base used in the determination as well as solvation effects.[12] These ambiguities could be of pivotal importance to the work of rationally designing chemical systems that rely on use of metal cations for tuning, particularly quantitative work in redox chemistry. This situation arises because of the observation that reduction potentials, for example, can be readily tuned in heterobimetallic complexes by exchanging incorporated metal cations.[2,9] For metal cations, a convenient scale of Lewis acidity that has emerged in recent years comes from Brønsted-Lowry acidity values, gathered together by Perrin in an important and comprehensive catalogue,[4] that are pK_a values of water bound to metal aqua complexes of corresponding metal cations of interest (pK_a of $[M(OH_2)_n]^{n+}$). Since water is assumed to be in vast excess relative to the metal cations, on the one hand pK_a values could be thought to reflect the electrostatic effect of binding water to a given metal cation. The pK_a values should not, on the other hand and contrary to our view, be viewed as *directly* reporting on the binding affinity between cations and water; the inner-sphere binding of water and any aqueous solvation effects are implicit in the measured pK_a values because the water molecules vastly outnumber the metal cations being studied in the measurements.

Systematic Trends between Titrations in MeCN and pK_a Values in H_2O

In light of this situation for the established pK_a scale, we were curious if there would be any systematic trends when comparing our quantified parameters from the titrations as a function of the aqueous pK_a descriptor. On the basis of the dynamic range differences that emerged in the titration studies of probes **E**, **O**, and **P**, this is of even higher interest. Here, we have found co-linear relationships between $\Delta\delta'_{max}$ and the relevant pK_a values; these relationships emerge for the probe molecules studied in this work, particularly for **E** and **P** (see Figure 3). While **E** and **O** have similar $\Delta\delta'_{max}$ values for every cation interrogated here, **P** has significantly smaller $\Delta\delta'_{max}$ values across the series compared to the other probes, highlighting the impact of the discrepancy in the dynamic ranges between **P** and the trialkyl phosphine oxides. In other words, the same ions can display apparently quite different measurements depending on the substitution pattern of the probe.

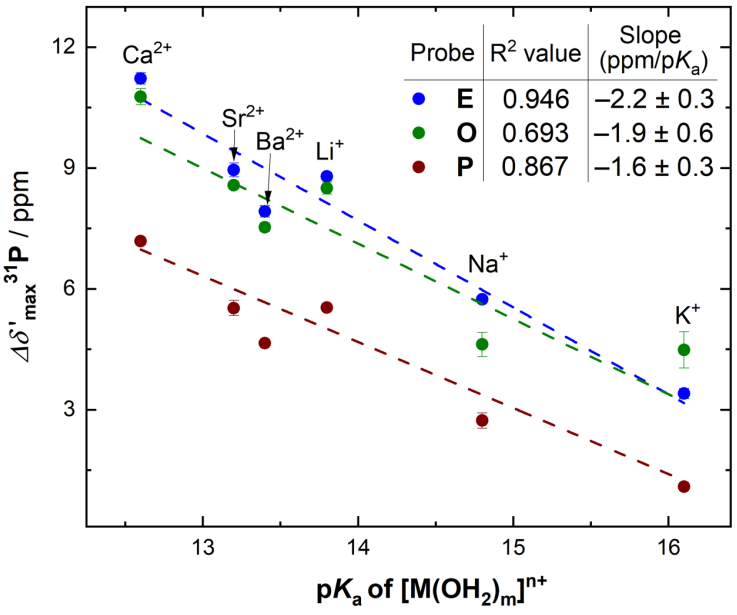

Figure 3. $\Delta\delta'_{max}{}^{31}$P values from Hill-Langmuir fit for titrations with all three probes plotted against the aqueous pK_a values of the corresponding metal-aqua complexes. Goodness of fit values (R^2) and slopes of the lines of best fit are shown for each probe dataset in the legend.

On the other hand, all three probes show an approximately equal tendency to show larger $\Delta\delta'_{max}$ values for metal cations with smaller pK_a values, demonstrated by the similarity of the slopes of the lines of best fit for all three datasets (given in Figure 3). This suggests that **E**, **O**, and **P** could all be equally useful in distinguishing the Lewis acidity of the cations. The linear correlation between $\Delta\delta'_{max}$ and the aqueous pK_a values in the cases of all three probe molecules suggests there are similarities between the aqueous and non-aqueous chemistries of the metal cations. This can be attributed here to the coordinating nature of MeCN, similar to that of H_2O. On the other hand, such co-linear behavior must be purely coincidental and, we feel, should not be taken as an indication that these solvents are "similar." This point of view is underscored by the much lower goodness-of-fit relationship (R^2 value) between $\Delta\delta'_{max}$ ^{31}P and pK_a for **O**, in that one would be less likely to conclude there is a strongly co-linear relationship between these parameters when using **O** as the probe molecule. The lower R^2 value for the **O** dataset may be due in part to an apparent overestimation of $\Delta\delta'_{max}$ for the titration of **O** with K^+ as judged by the fit to the HLE. However, there could be more uncertainty in the $\Delta\delta'_{max}$ values for weakly acidic cations like K^+, as these ions display very low binding affinity for the phosphine oxide probes (see Table 1). For example, in the data corresponding to **O** titrated with KOTf, the fitted $K_{1/2}$ value from the HLE predicts that upwards of 0.45 M KOTf is needed to attain measured $\Delta\delta$ values that would be nearly equal to $\Delta\delta'_{max}$. However, this finding also bears resemblance to the very weak or even non-acidic behavior of K^+ under aqueous conditions.[20]

The correlation between $\Delta\delta'_{max}$ for the individual metal cations and the pK_a values of the corresponding metal aqua complexes is supported by the notion that $\Delta\delta'_{max}$ represents an estimation of the chemical shift of the probe when it is maximally bound to a given metal cation. However, the comparison of **E**, **O**, and **P** in this work also affords the opportunity to interrogate

how the binding strength of the individual probe molecules to the metal cations may be influenced by the properties of those cations. Binding strength was quantified here with the $K_{1/2}$ values arising from fitting our data to the HLE because $K_{1/2}$ values could be produced for both the mono- and divalent ions. Plotting the $K_{1/2}$ values obtained from the HLE as a function of the pK_a values of the corresponding $[M(OH_2)_n]^{n+}$ reveals that the more strongly Lewis acidic metal cations (as judged by the aqueous behavior) bind more tightly to **E**, **O**, and **P** than their weaker counterparts (see Figure 4). Furthermore, fairly linear relationships for all three probes could be obtained here by plotting $K_{1/2}$ on a logarithmic scale (of the form $\log(K_{1/2})$). The linearity of the relationships suggests that the binding of the phosphine oxide probes to the metal cations becomes increasingly thermodynamically preferred as the charge density of the metal cation increases. We anticipate that this behavior is due in part to the polar aprotic nature of MeCN, which is not able to solvate highly charged species as effectively as water.

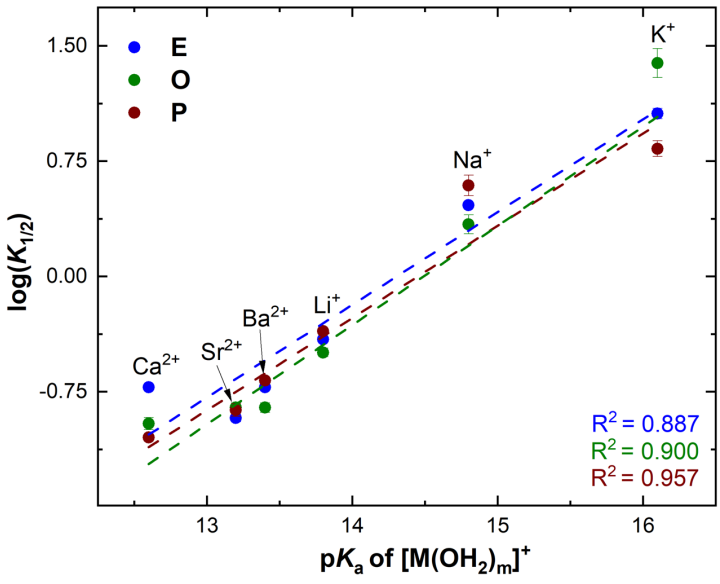

Figure 4. $\log(K_{1/2})$ values from fitting titration data of all three probes to the HLE, plotted against the pK_a values of the corresponding metal-aqua complexes.

In light of the apparent correlation between $K_{1/2}$ obtained from our Gutmann-Beckett-like titrations and the pK_a values of $[M(OH_2)_n]^{n+}$, one might expect that the more electron-rich **E** and **O** would bind more tightly to metal cations when compared to **P**. However, there are no significant systematic differences between **E**, **O**, and **P** in their overall binding affinities to the metal cations interrogated here, as judged by the $K_{1/2}$ values. We anticipate on the basis of these findings that the effect of the various substituents on the binding of the probe molecules to the metal cations is simply too minor to be detected in this work. This can be visualized in the data in Figure 4, where there is no systematic ordering of the probe molecules within the results for each cation. Thus, the overall thermodynamics of the cation-probe binding events measured here can be primarily ascribed to the identities of the Lewis acidic metal cations used in each case. From this perspective, the phosphine oxide probes behave with similar properties, as dictated by the presence of a structurally similar [P–O] core in each case.

On the other hand, the identity of the probe does impact the nature of the "cooperativity" displayed by each probe. There is a clear trend between the "cooperativity" values from our measurements and the aqueous pK_a values. As shown in Figure 5, the binding of weaker Lewis acids (K^+ and Na^+) with all three probes is essentially non-cooperative, with α values measured for all the probes being tightly clustered near 1.0; this finding is in line with the established 1:1 probe:cation binding equilibria for these ions (*vide supra*). On the other hand, the stronger Lewis acids (Li^+, Ba^{2+}, Sr^{2+}, and Ca^{2+}) bind to the probes with noticeable positive cooperativity that increases as a function of the aqueous pK_a values associated with the metal complexes. Moreover, within the data for these four cations, **E** and/or **O** display more noticeably positive "cooperativity" than does **P**. A possible conclusion is thus that use of stronger Lewis acids or stronger Lewis bases in these titrations drives an increase in the "cooperativity" of the solution behavior. From the

standpoint of the metal cations, Ca^{2+} would be anticipated to be the strongest Lewis acid on the basis of charge density and/or its pKa value in water; thus, it displays the highest cooperativity values among all the ions studied here. Similarly, when **E** and/or **O** are compared to **P**, those probes display higher cooperativity when titrated with the same metal ions. This suggests that the general notion of Lewis acidity (as judged by the workhorse pK_a values) is correlated to the nature of the equilibria present (measured by α) between the phosphine oxide probes and the metal cations examined here. This correlation emphasizes that the tendency of a given probe to bind multiple metal cations is increased when that probe itself is more electron rich and thus a stronger Lewis base, and that use of a stronger Lewis acid can result in more pronounced binding of multiple cations to its given paired base.

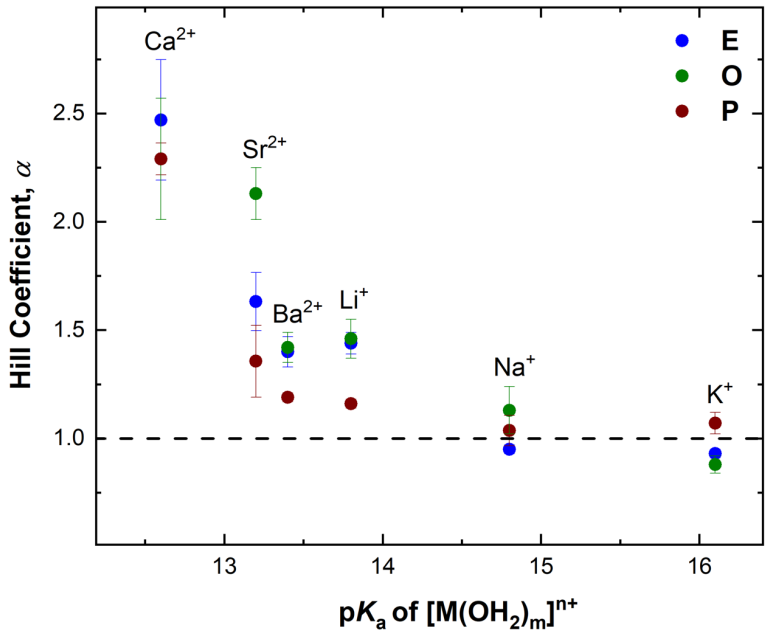

Figure 5. Hill coefficient (α) values for titrations with all three probes plotted against the pK_a values of the corresponding metal-aqua complexes.

Investigation of Counter-anion Influences via Titrations

In light of these electrostatic considerations, an additional factor that could impact these findings is speciation associated with the triflate counter-anions.[21] Such influence could arise in the polar aprotic solvent MeCN from formation of solvated ion pairs or triflate-bound metal complexes. Triflate could be found in the inner or outer coordination sphere, or could be completely free in solution, giving numerous options that could differ between ions as well. To estimate whether these behaviors influence our data, titrations of **E** were carried out with the monovalent hexafluorophosphate (PF_6^-) salts of Li^+, Na^+, K^+, and Cs^+, as well as sodium tetrakis(3,5-bis(trifluoromethyl)phenyl)borate ($NaBArF_{24}$).

As in the case of the triflate salts described earlier in this paper, the salts of PF_6^- and $BArF_{24}^-$ were used only after extensive drying (heating *in vacuo* for 24 h) and after characterization by IR and ^1H, ^{19}F, and other heteronuclear NMR spectroscopies to confirm purity (see Supporting Information, Figures S65-S75). KPF_6, $NaPF_6$, and $LiPF_6$ were purchased from Strem Chemicals and were found to be sufficiently pure for use after drying. $CsPF_6$, however, is not commercially available and thus was prepared via treatment of cesium carbonate with hexafluorophosphoric acid (HPF_6), and was used only after extensive drying (see Experimental Section) and characterization (see SI, Figures S65 and S71). $NaBArF_{24}$ was prepared according to literature procedures[22] with the guidance of a detailed protocol assembled by the Peters Group.[23]

We were excited to find that titrations of **E** with the PF_6^- salts of the Li^+, Na^+, K^+, and Cs^+ provided readily interpretable data in all cases. Much like in the cases of the triflate salts, a single ^{31}P probe signal migrates downfield with increasing cation-to-probe ratios. Furthermore, much like titrations of **E** with the triflate salts, more charge-dense cations gave rise to larger $\Delta\delta$ values at any given metal/probe ratio as compared to the less charge dense, weaker Lewis acids (see Figure 6).

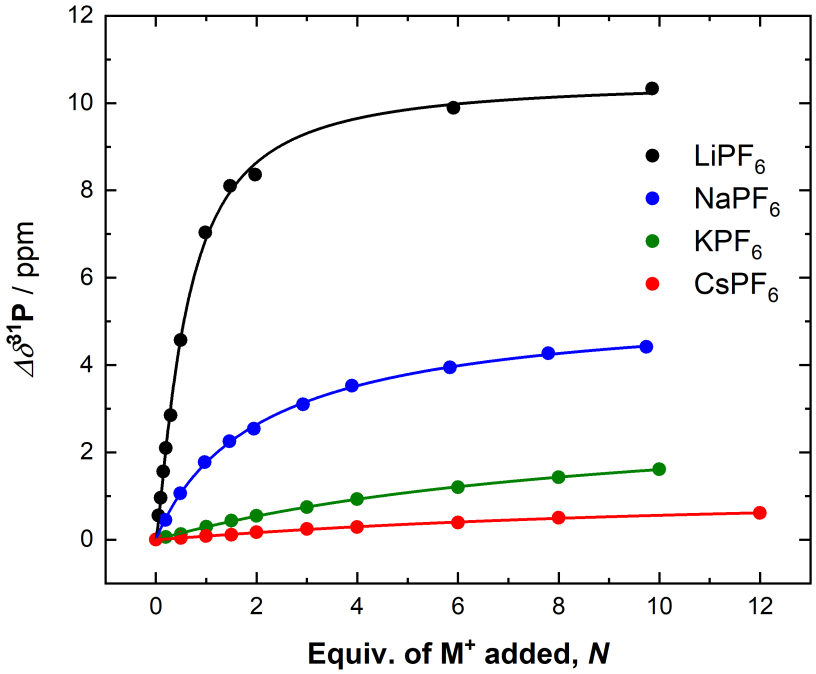

Figure 6. $\Delta\delta^{31}$P values plotted against equivalents of added hexafluorophosphate salts of monovalent metal ions for titrations with **E**. Curves shown are fit with the Hill-Langmuir equation.

The $\Delta\delta_{max}$ values are similar across the titrations of NaOTf, $NaPF_6$, and $NaBArF_{24}$ (see Supporting Information, Figure S83), as well as for the titrations of KOTf and KPF_6 (see Supporting Information, Figure S82). These findings indicate that the identity of the counter-anion does not have a significant impact on the electrostatic interactions between the larger monovalent cations and **E** in MeCN. The titrations of **E** with $NaPF_6$, and $NaBArF_{24}$ reveal similar values of K_a (from fitting to the 1:1 binding isotherm equation) and $K_{1/2}$ (from fitting to the HLE), as shown in Table 3. On the other hand, we did find that there is slightly weaker binding of Na^+ to **E** in the case of NaOTf as compared to the cases of $NaPF_6$ and $NaBArF_{24}$ (see Table 3 for $NaPF_6$ and $NaBArF_{24}$ data and Table 1 for NaOTf data). For the weaker Lewis acid K^+, binding affinity to **E** is virtually unaffected by the identity of the counter-anion, whether it be OTf^- or PF_6^-. Moreover, all the

titrations with Na^+ and K^+ with **E** suggest a 1:1 binding stoichiometry, regardless of the identity of the counter-anion.

Table 3. Fitted parameters for the full titrations of **E** with hexafluorophosphate salts and $NaBArF_{24}$.

Equation Used	Parameters	$LiPF_6$	$NaPF_6$	KPF_6	$CsPF_6$ [b]	$NaBArF_{24}$
1:1 Isotherm Equation	K_a (M^{-1}) [a]	—	74.67 ± 5.42	11.46 ± 0.46	10.33 ± 1.16	63.26 ± 1.77
	$\Delta\delta_{max}$ ^{31}P (ppm) [a]	—	5.00 ± 0.10	3.04 ± 0.07	1.34 ± 0.10	4.94 ± 0.04
Hill-Langmuir Equation	$\Delta\delta'_{max}$ ^{31}P (ppm) [a]	10.53 ± 0.14	5.47 ± 0.12	3.06 ± 0.20	1.14 ± 0.17	5.18 ± 0.03
	$K_{1/2}$ (equiv.) [a]	0.60 ± 0.02	2.16 ± 0.12	9.03 ± 1.09	10.32 ± 2.72	2.26 ± 0.03
	α [a]	1.27 ± 0.04	0.96 ± 0.03	1.02 ± 0.03	1.10 ± 0.08	1.03 ± 0.01

[a] Errors were calculated from the direct nonlinear fit of equations 1 and 2 and are given as ±1σ. [b] The titration of **E** with $CsPF_6$ was carried out at a constant probe concentration of 7.3 mM (instead of 10 mM as in the other cases). This was necessitated by the limited solubility of $CsPF_6$ in MeCN and the need for large excesses of Cs^+ with respect to the **E** for a proper estimation of $\Delta\delta_{max}$.

Similar to these findings for Na^+ and K^+, the data suggest 1:1 binding of Cs^+ and **E**, based on the reasonable fit provided by the 1:1 binding isotherm (see SI, Figure S85) and the closeness of α (from the fit to the HLE; see Figure 6) to unity. As Cs^+ is the weakest Lewis acid tested in this work, the small $\Delta\delta'_{max}$ value for the titration of **E** with $CsPF_6$ and the weak binding affinity between Cs^+ and **E** are in line with the correlations between $\Delta\delta'_{max}$ and $K_{1/2}$ with the pK_a values of $[\mathbf{M}(OH_2)_n]^{n+}$ as discussed above.

Looking at the case of the smaller Li^+ ion, however, there was a much greater difference in the appearance of the titration data for **E** with $LiPF_6$ compared to LiOTf. Fitting of the data for $LiPF_6$ to the HLE gives significantly larger $K_{1/2}$ values (0.60 vs. 0.39, respectively) and $\Delta\delta'_{max}$ values (10.53 vs. 8.79) for this salt in comparison to LiOTf. Thus, the hexafluorophosphate salt of lithium appears to be a significantly stronger Lewis acid in comparison with its triflate salt. This finding suggests that triflate is likely bound more tightly to the small lithium cation in solution, either within the first or perhaps second coordination sphere. This hypothesis is supported by the

behavior of the other cations in this study, in that the stronger Lewis acids should have more favorable thermodynamics of triflate binding than the weaker cations. And, triflate can be reasonably anticipated to be a stronger Lewis base than hexafluorophosphate. As an aside, during the course of execution of this work, inspection of the literature revealed that surprisingly little quantitative data is available regarding the stability and speciation properties of $LiPF_6$, despite the importance of this compound as the "gold standard" electrolyte for use in lithium-ion batteries[24] and its recognized tendency to react with water.[25,26] Reactivity of this salt with water is a major challenge, in that one known product of hydrolysis, HF, is quite corrosive, and that the full speciation profile resulting from reaction with H_2O is highly dependent upon the conditions used for the studies. In light of these issues, some reports appear to be of meager quality.[26]

Comparison of Mono-, Di-, and Trivalent Metal Cations

With all of these findings in hand, our final approach to comparison of the ability of **E**, **O**, and **P** to quantify Lewis acidity in MeCN was investigation of a broader range of metal cations, particularly including more challenging trivalent rare earth cations and the uranyl ion. In our previous work,[9] additions of 1 equivalent of such strong Lewis acids to **P** resulted in multiple probe signals in $^{31}P\{^1H\}$ NMR spectra, indicating the formation of multiple persistent species. Slow exchange between these various species precludes satisfactory fitting of full titration data sets to either the 1:1 binding isotherm or the HLE. Here, we carried out single-point $^{31}P\{^1H\}$-NMR measurements with 1:1 mixtures of a wide range of metal cations with **E**, **O**, and **P** in order to *i)* observe broader trends in the data across classes of metal cations and *ii)* track the behavior of the probe molecules in the sort of single-point measurements commonly used in the field.

When plotted against the relevant pK_a values measured in water,[4] the measured $\Delta\delta$ values of the 1:1 mixtures of probe and cation revealed strikingly linear relationships for all the probes (see Figure 7). Recapitulating the findings from the individual titrations, **E** and **O** behave similarly and display significantly greater dynamic ranges than **P**. This observation can be understood, however, on the basis of the titration data to arise not from systematic differences in association constants for the various probes, but rather due to an intrinsic difference in the electron-nuclear interactions in **P** compared to **E** and **O**. The data reveal that the slopes of the lines of best fit for $\Delta\delta$ vs. pK_a are the same for **E** and **O**, but significantly smaller for **P**: –2.7, –2.7, and –1.8, respectively. The difference in slope between **E**/**O** and **P** is attributable to the difference between individual $\Delta\delta$ values that increases with Lewis acidity; the data for Na^+ with all the probes is not significantly different, but the gap between the $\Delta\delta$ values for **E**/**O** vs. **P** grows when plotted as a function of the aqueous pK_a values.

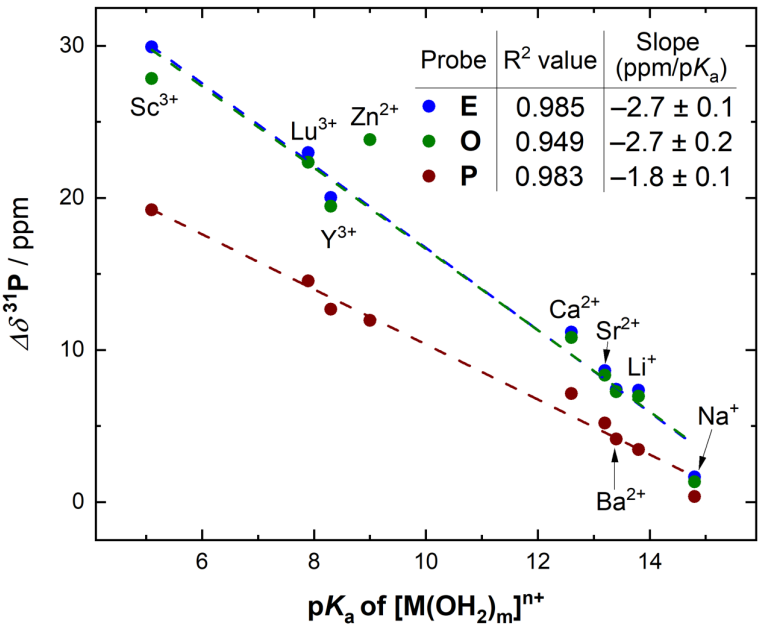

Figure 7. $\Delta\delta^{31}$P values from 1-to-1 mixtures of metal ion and probe molecule for all three probes, plotted against the pK_a values of the corresponding metal-aqua complexes. Goodness of fit values (R^2) and slopes of the lines of best fit are shown for each dataset. [**M**] = [probe] = 10 mM. Solvent: MeCN.

These unique slopes contrast with the indistinguishable values found when plotting $\Delta\delta'_{max}$ against pK_a (see Figure 3) where all three probes showed similar tendencies to give larger $\Delta\delta'_{max}$ values with increasing Lewis acidity. In the single point measurements, the relatively low binding affinity between the probe molecules and weak Lewis acids (e.g. Na^+) causes an understatement of the differences in the intrinsic dynamic ranges of the probes; since little Na^+ is bound to any of the probe molecules when only 1 equivalent is present, the $\Delta\delta$ values from single point measurements are close to zero regardless of dynamic ranges of the probes. However, for metal cations which bind very tightly to phosphine oxides, differences in $\Delta\delta$ between single-point measurements using **E**, **O**, and **P** become pronounced since $\Delta\delta$ more closely approaches the ultimate value of $\Delta\delta'_{max}$. It appears, thus, that there is a multiplicative interplay between binding affinity and dynamic range that ultimately determines the outcome of the single-point measurements of Lewis acidity. $\Delta\delta$ values from single-point measurements become better reporters of the electrostatic interactions between metal cations and probe molecules as the binding affinity increases and $\Delta\delta$ approaches $\Delta\delta'_{max}$. Additionally, as quantified with the Hill coefficient from the fitting of titrations data to the HLE, **E** and **O** have a greater propensity to bind multiple metal cations compared to **P** (see Table 2 and Figure 5). Thus, even in the presence of 1 equivalent of metal cation, the trialkyl phosphine oxides could, on average, be bound to more cations at one time compared to the less "cooperative" **P**. This could also contribute to the larger $\Delta\delta$ values for **E** and **O** compared to **P**.

Previously, we estimated the pK_a values of K^+, Rb^+, and Cs^+ using the line of best fit for the plot of $\Delta\delta$ vs. pK_a with **P**. Aside from this determination, there have been various pK_a measurements for these very weakly Lewis acidic cations in the past,[4] but the available prior data are in conflict with one another, in that a range of previously determined values are available for use. We suspect

the apparent difficulty of these measurements arises from the negligible change in the pH of water upon dissolution of these weakly acidic cations. The sensitivity of the Gutmann-Beckett-type measurements reported here, however, allows for an estimation of pK_a extrapolated from the dependence of $\Delta\delta$ on pK_a for other cations for which more reliable measurements of pK_a are available in the Perrin catalogue.[4] Using the lines of best fit shown in Figure 7, we thus estimated the pK_a values of K^+, Rb^+, and Cs^+ with **E**, **O**, and **P**. We also measured the Lewis acidity of the uranyl dication (UO_2^{2+}) in the form of its triflate salt (see Table 3 for all the new values) for comparison to the known tendency of the uranyl cation to acidify water.

Table 3. Estimation of Brønsted acidity of metal-aqua complexes based on $\Delta\delta^{31}$P values from 1-to-1 mixtures of metal ion and probe molecule. pK_a values were calculated with linear extrapolation using the lines of best fit shown in Figure 7.

Triflate Salt	Probe	$\Delta\delta^{31}$P [a]	Estimated pK_a [b]
CsOTf	**E**	0.10	16.1 ± 1.0
	O	0.09	16.2 ± 1.7
	P	0.04	15.7 ± 1.0
RbOTf	**E**	0.16	16.1 ± 1.0
	O	0.12	16.2 ± 1.7
	P	0.04	15.7 ± 1.0
KOTf	**E**	0.41	16.0 ± 1.0
	O	0.23	16.1 ± 1.7
	P	0.09	15.7 ± 1.0
$UO_2(OTf)_2$ [c]	**E**	32.95	4.0 ± 0.6
	O	33.09	3.8 ± 1.0
	P	23.89	2.5 ± 0.6

[a] Measured with [cation] = [probe] = 10 mM. [b] Errors on the estimated pK_a values were derived from the uncertainty on the linear fit of the relationships between pK_a and $\Delta\delta^{31}$P as shown in Figure 7. [c] The experimentally determined pK_a of H_2O bound to the uranyl ion is 5.8, as given in reference 4.

We were encouraged to see that estimates of pK_a for K^+, Rb^+, and Cs^+ were similar for all three probes. Despite the small $\Delta\delta$ values associated with the addition of one equivalent of these weak Lewis acids, a reproducible estimation of pK_a is achieved. The estimates of the pK_a value of UO_2^{2+} using **E**, **O**, and **P** were all dramatically lower, however, than the established literature value of 5.8.[4] The deviation from the expected $\Delta\delta$ value produced by UO_2^{2+} is most pronounced for **P**, while **E** and **O** gave similar results. As mentioned previously, $\Delta\delta$ values for 1:1 mixtures of probe

and cation depend on multiple factors, including binding affinity. The very low estimated pK_a values of UO_2^{2+} in MeCN from these single point measurements are likely attributable to the anticipated large association constants for binding UO_2^{2+} to phosphine oxides; phosphorus-based reagents/ligands have indeed found broad utility in schemes for separation involving lanthanides and actinides (An).[27] The presence of the two tightly bound oxo ligands and the large coordination sphere of UO_2^{2+} also distinguishes it from the other cations featured in this study, features that likely engender unique speciation behavior that could give rise to large $\Delta\delta$ values. In any case, it is clear from the measured values that the uranyl ion can function as a strong Lewis acid in MeCN, particularly when formulated as its triflate salt.

DISCUSSION

When titrated with monovalent and divalent cations, **E**, **O**, and **P** all give systematic and interpretable plots of $\Delta\delta$ against equivalents of M^{n+} added. For all three probes, $\Delta\delta'_{max}$ values from full titrations with K^+, Na^+, Li^+, Ba^{2+}, Sr^{2+}, and Ca^{2+} are linearly correlated with the pK_a values of the corresponding $[\mathbf{M}(OH_2)_n]^{n+}$. Broadly, these linear relationships suggest Lewis acidity in water has a corresponding relationship with effective Lewis acidity in MeCN as measured by phosphine oxide probe molecules **E**, **O**, and **P**. As such, we anticipate that pK_a values of $[\mathbf{M}(OH_2)_n]^{n+}$ can be helpful predictors of the electrostatic influence of secondary metal cations, even when these are judged with data from disparate experimental conditions.

The larger dynamic range of **E** and **O** as compared to **P** (as shown most clearly in Figure 3) suggest that the electron-nuclear interactions at the ^{31}P center in **E** and **O** are more susceptible to perturbation upon cation binding as compared to **P**. The difference in dynamic range between the alkyl probes and the aryl probe studied here coincides with the order of the ^{31}P chemical shifts of

the bare probes in MeCN; **E** gives a signal that is the most downfield (48.6 ppm), the ^{31}P signal for **O** is slightly further upfield (44.9 ppm), and **P** gives a signal that is much further upfield (25.1 ppm). From the theory of NMR spectroscopy,[18] the solution-phase symmetry of the phosphine oxides discussed in this work (C_{3v} point group in all cases) can be thought to give rise to anisotropic electron distributions about phosphorous and thus multiple chemical shift tensor elements that contribute to the measured isotropic chemical shift of the probes. There are two limiting orientations (parallel and perpendicular to the P–O moiety) of the chemical shift tensor elements that define the properties of the ^{31}P center, as shown in Figure 8. Here, we hypothesize that the chemical shift tensor elements oriented along the P–O bonds ($\sigma_{parallel}$) in **E**, **O,** and **P** are those affected by the binding of a metal cation to the terminal oxygen. Within this model, the identity of the substituents on the probe would affect the intrinsic properties of the probe molecule, but the tensor elements perpendicular to the P–O bonds ($\sigma_{perpendicular}$) would be less affected by cation binding. The measured dynamic range difference then suggests that the substituents affect the properties of the P–O moiety, and thereby influence $\sigma_{parallel}$ in addition to $\sigma_{perpendicular}$. This hypothesis is in agreement with a recent computational prediction from Greb and co-workers[12] that the properties of the P–O bond govern the interaction of probe species with Lewis acids.

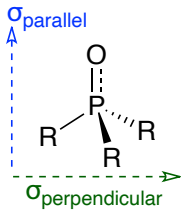

Figure 8. The two limiting chemical shift tensor element orientations for trisubstituted phosphine oxides are shown; $\sigma_{parallel}$ (shown in blue) is oriented along the P—O bond, while $\sigma_{perpendicular}$ (shown in green) is oriented orthogonally to the P—O bond.

Vibrational and structural data provide evidence to support this hypothesis. Infrared spectra of **E** and **O** reveal lower frequency P–O stretches (1157 cm^{-1} and 1144 cm^{-1}, respectively) in comparison to that of **P** (1188 cm^{-1}; see SI, Figure S91). Thus, the P–O bonds in the trialkyl derivatives are less rigid than those in the more electron deficient **P**. This could explain the greater dynamic range exhibited by the trialkyl phosphine oxides, in that the P–O bonds in the more electron-rich probes could readily undergo more substantial changes upon binding of metal cations. Similarly, structural data from X-ray diffraction analyses of **E**, **O**, and **P** are available in the Cambridge Structural Database (CSD),[28] and these offer quantitative data on the P–O distances in the probe molecules when not bound inner-sphere to metal cations. There are three suitable structures of **E** available,[29,30,31] one of **O**,[32] and three of **P**.[33,34,35] Averaging together the available data for each probe, the P–O distances in **E**, **O**, and **P** are 1.495(4), 1.495(1), and 1.485(2) Å, respectively.[36] These data show that the P–O distances in **E** and **O** are virtually indistinguishable, a finding in accord with the similar inductive properties of the ethyl and octyl groups present in these probes. However, the P–O distance in **P** is marginally shorter (Δd = 0.01 Å) than in the other two probes, suggesting that the greater electron richness in **E** and **O** indeed contributes to a longer, weaker bond between the central P atom and the terminal oxo. Taken together with the vibrational data suggesting weaker P–O bonds in **E** and **O** vs. **P**, it appears that less rigid P–O bonds in trialkylphosphine oxides are associated with greater dynamic ranges in these ^{31}P NMR molecular probes of Lewis acidity.

The behavior of **E**, **O**, and **P** as probe molecules can be further distinguished beyond considerations related to dynamic range. First, we find that the linewidth of the ^{31}P signal can vary at a given metal-to-probe ratio depending on the identity of the probe. The trialkylphosphine oxides give sharper ^{31}P signals (as judged by the measured FWHM values) for trivalent cations like Y^{3+}

(see SI, Figure S93 and Table S5), with the result that the ^{31}P signals of **P** tend to appear less distinctly when **P** is bound to these highly charged ions. On the other hand, **P** can be viewed as a more desirable probe than **E** or **O** under different conditions; **E** and **O** give quite broad signals at certain metal-to-probe ratios with the divalent cations like Ca^{2+} and Zn^{2+} (See SI, Figures S92 and S94). Consequently, different probe molecules can be useful depending on the context; if one measurement condition is required but a given probe does not return useful data, a different probe molecule could be selected which might provide improved data quality.

Finally, as shown in Figure 5, **E** and **O** generally display greater deviations from 1:1 binding than **P**. At first glance, this can be attributed to a greater propensity for these more electron rich probes to simultaneously bind multiple cations, giving rise to the "positive cooperativity" manifested in the titration data shown in Figure 2. As originally developed in the context of enzymology, the concept of "positive cooperativity" applies to systems in which the binding of substrates (here, metal cations) becomes more favorable after the initial binding of one substrate changes the properties (usually conformation or solvation) of the "host" (here, the probe). Using a linearized form of the HLE given in equation (3), the equilibrium constants of the first and last possible events can be estimated in order to provide a measure of the difference in Gibbs free energy change ($\Delta\Delta G$) of the two binding events, a quantity known in the field as interaction energy. Notably, in positively cooperative systems, the equilibrium constant of the final binding event (K_x) is greater than that of the first event (K_y).[37]

$$\log\left[\frac{\Delta\delta}{\Delta\delta'_{max} - \Delta\delta}\right] = \alpha \log N - \alpha \log K_{1/2} \quad (3)$$

To analyze the data presented here in this manner, we tabulated the interaction energies for Ba^{2+}, Sr^{2+}, and Ca^{2+} using extrapolated tangent lines at the extrema of the linearized HLE plots (See SI, Figure S95); the values are given in Table S6.

Plotting the tabulated values as a function of the corresponding aqueous pK_a values of the metal cations reveals that interaction energy appears to be related to the charge densities of the metal cations (see Figure 9). With all three probes, it appears that the smallest and most charge dense cations are most aggressive in multiple binding to a single phosphine oxide. Indeed, the roughly co-linear relationships between pK_a and the values of interaction energy shown in Figure 9 illustrate that increasing Lewis acidity is associated with larger interaction energies. This is consistent with the Hill coefficient (α) values given in Figure 5 and is a feature attributable to the greater electron density about oxygen in **E** and **O** compared to **P** (i.e., greater basicity/electron-richness about oxygen in **E** and **O** compared to **P**). The more flexible alkyl groups about the probes **E** and **O** could also play a role; the more rigid phenyl groups of **P** are presumably less susceptible to coordination-induced reorganization that could drive changes in probe affinity upon binding of the first metal cation.

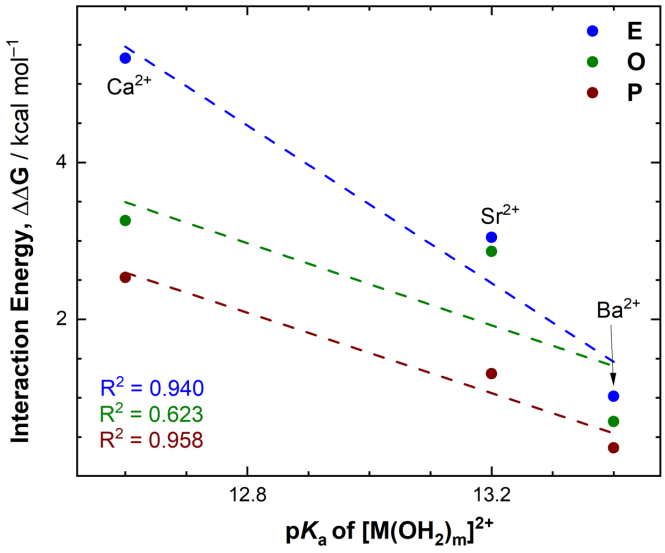

Figure 9. Apparent interaction energy of divalent ion binding to all three probes plotted against the pK_a values of the corresponding metal-aqua complexes.

However, in order for the calculated values of interaction energy to report quantitatively on the equilibria operative during probe-cation binding, instrument response (in this case, $\Delta\delta^{31}$P) must be directly proportional to the concentration of the metal cation that is bound to the probe molecule. When 1:1 binding strictly applies, $\Delta\delta$ is *directly proportional* to the concentration of probe-cation adduct, and thus $\Delta\delta'_{max}$ *does reflect* the chemical shift of the probe molecules when bound to a single cation. However, for systems where multiple equilibria occur, the induced de-shielding of the ^{31}P NMR signal of a probe upon binding of a single cation to a probe molecule *cannot* be concluded (on the basis of the data available here) to be equivalent to the de-shielding effect of binding a second (or third) cation. Thus, $\Delta\delta$ in our NMR measurements with the di- and tri-valent cations is *not linearly related* to the concentration of metal cations bound to probe molecules; thus the tabulated values given in Table S6 represent *apparent interaction energies* that report on both *i)* the association constants for equilibria operative in each system and *ii)* the magnitude of the change in chemical shift of the probe ^{31}P signal that results from formation of each of the individual species present in the overall set of equilibria. On the one hand, these findings underscore that the calculated apparent interaction energies do not reflect the actual relative energetics of probe-cation adduct formation. On the other hand, however, they highlight that the "cooperativity" effects quantified by fitting to the HLE are best considered multi-equilibrium effects in our work, and that stronger Lewis acids have a greater propensity to bind multiple phosphine oxide probe molecules.

And, finally, we note here that the HLE provides an appealing approach to measurement of speciation of these metal cations in MeCN. It appeals as it is applicable to all of the phosphine oxide probes that we have tested so far, and as it enables a harmonized, quantitative window into probe-cation adduct formation that can be applied across the various probes and various metal cations. We feel that it represents a valuable approach, particularly for quantification of Lewis

acidity properties of the homologous series of metal triflate salts. We anticipate that further explorations into the properties of more structurally diverse probes could unlock the ability to use the HLE to fully interrogate the properties of trivalent cations in solution, an important research goal as such cations remain challenging to handle in the context of separations science and broader applications in multimetallic systems.

CONCLUSIONS

Comparing the phosphine oxide probe molecules examined in this study in MeCN, **E** and **O** display a markedly wider dynamic range than **P**, a feature that could motivate expanded use of these probes in future studies relying on Gutmann-Beckett-like measurements. On the other hand, **E**, **O**, and **P** present unique speciation behavior and exchange properties with certain metal cations and at specific cation-to-probe ratios, highlighting the utility of developing a toolkit of multiple probes for estimating Lewis acidity properties under diverse conditions. All three probes studied here are suitable for use with strong Lewis acids like the trivalent rare earth cations as well as the uranyl dication, illustrating the high charge density of these ions in MeCN and building on prior work carried out in aqueous media. The triflate anion, often considered to be weakly coordinating but capable of inner-sphere coordination nonetheless, does not appear to strongly influence the binding of metal ions to phosphine oxides in MeCN, as PF_6^- and $BArF_{24}^-$ salts appear similar to their triflate analogues in several cases studied here. Taken together, this work suggests that exploration of even more electronically distinctive phosphine oxides could unlock new analytical opportunities and afford new insights into the speciation properties of challenging cations, particularly among the important rare earths and actinides.

EXPERIMENTAL SECTION

General Considerations

Trioctylphopshine oxide (**O**; Fischer Scientific, 98%), triethylphosphine oxide (**E**; Fischer Scientific, 98%), and triphenylphosphine oxide (**P**; Fischer Scientific, 99%) were found to be air-stable but were nonetheless immediately dried *in vacuo* at 30°C for 24 hours before storing in the inert atmosphere glovebox. All the commercially available triflate salts were purchased from Strem Chemicals and were used after drying *in vacuo* at 180°C for 24 hours. Potassium, sodium, and lithium hexafluorophosphate (KPF_6, $NaPF_6$, $LiPF_6$) were purchased from Strem Chemicals and dried *in vacuo* for 24 hours (the former two at 180°C as received and the latter at 140°C after recrystallization from MeCN and Et_2O).

All manipulations were carried out in dry N_2-filled gloveboxes (Vacuum Atmospheres Co., Hawthorne, CA) or under N_2 atmosphere using standard Schlenk techniques unless otherwise noted. All solvents were of commercial grade and dried over activated alumina using a PPT Glass Contour (Nashua, NH) solvent purification system prior to use, and were stored over molecular sieves. All chemicals were from major commercial suppliers and used only after extensive drying. CD_3CN was purchased from Cambridge Isotope Laboratories (Tewksbury, MA, USA) and dried over 3 Å molecular sieves.

^1H, ^{31}P, and ^{19}F NMR spectra were collected on a 400 MHz Bruker spectrometer (Bruker, Billerica, MA, USA). Chemical shifts (δ) are reported in units of ppm and coupling constants (J) are reported in Hz. All experiments were conducted at room temperature (298 K). ^1H spectra were referenced to the residual protio-solvent signal.[38] ^{31}P and ^{19}F NMR spectra were referenced and reported relative to H_3PO_4 and CCl_3F, respectively, as external standards following the scale recommended by IUPAC[17] based on ratios of absolute frequencies (Ξ). ^{31}P NMR spectra in MeCN

were referenced relative to tetrabutylammonium hexafluorophosphate ($TBAPF_6$) which served as an external standard in sealed capillary tubes; the spectra are reported relative to H_3PO_4. Under these conditions, $TBAPF_6$ displays a septet in ^{31}P NMR centered at ca. –145.6 ppm. Individual error values in this report are based upon numerical fits to multipoint datasets unless otherwise noted.

Infrared (IR) spectra were collected under an inert atmosphere in a dry N_2-filled glovebox (Vacuum Atmospheres Co., Hawthorne, CA). Spectra were collected with a Shimadzu IRSpirit FTIR spectrometer equipped with a QATR-S single-reflection attenuated total reflectance (ATR) accessory and diamond prism plate. Solid samples of the dried triflate salts were interrogated (see Supporting Information).

Following the general concept of Gutmann-Beckett method, where triethylphosphine oxide (TEPO) is commonly used as a probe molecule, we also used triphenylphosphine oxide (TPPO) and trioctylphosphine oxide (TOPO) as probes. Under inert atmosphere in a glovebox, a weighing balance (with 0.1 mg precision) was used to prepare samples containing probe molecules and the desired triflate salt. For ^{31}P NMR measurements of Lewis acidity, solutions of the triflate salts were prepared in MeCN; subsequently, varying volumes (ranging from 30 μL to 1000 μL) of these standard triflate salt solutions were then added to a solution of desired probe molecule via a Hamilton microsyringe. When needed, serial dilutions of the standard triflate salt solutions were used to execute small additions of metal ions to probe molecule solutions. To maintain constant concentrations of probe molecule across each titration, the mixtures of triflate salt and probe molecule were diluted with MeCN such that the final concentration of the probe was 10 mM. The $^{31}P\{^1H\}$ NMR shifts for the probe molecule were recorded; the chemical shifts are reported here

with an accuracy of 0.01 ppm. Our group has found that this level of accuracy is appropriate, based on external referencing studies.

Synthesis and characterization

Synthesis of $CsPF_6$. A Teflon round bottom flask was loaded with cesium carbonate (Cs_2CO_3, 5.0 g, 15.3 mmol) and water, forming a turbid solution. Under a blanket of N_2, hexafluorophosphoric acid (HPF_6, 4.95g, 23.9 mmol) was added dropwise to the suspension. After the addition was complete, the reaction mixture was stirred at room temperature for 1 h. Water was then evaporated, leaving an off-white solid. The solid was extracted with MeCN to remove unreacted Cs_2CO_3. MeCN was evaporated to give a white powder, and this was dried in vacuo at 180°C for 24 h. The product was used without further purification. Yield: 67% (4.45 g).

Synthesis of $UO_2(OTf)_2$. $UO_2(OTf)_2$ was synthesized by following a modified literature procedure.[16] A dry 50-mL Schlenk flask was loaded with uranium trioxide (UO_3, 0.954 g, 3.33 mmol) and degassed water (15 mL), forming a suspension. Under an inert atmosphere of N_2, triflic acid (CF_3SO_3H, 5.0 g, 33.3 mmol) was added with stirring to the suspension. After the addition was complete, the reaction mixture was refluxed at 110°C for 2 h. The resulting clear solution was distilled under reduced pressure first at 60°C to remove water and then at 190°C to remove excess triflic acid. The resulting pale-yellow solid was dried *in vacuo* at 180°C for 24 h, and then stored in the glovebox and used without further purification.

Quantification of H_2O in MeCN Solvent. To quantify the concentration of water in the MeCN solvent used in this work, we employed calcium hydride for stoichiometric generation of H_2 from any trace water that could be present after drying (assuming 1 eq. H_2 produced per 1 eq. H_2O in the sample). Analysis of gas samples was performed with a Shimadzu GC-2014 Custom-GC gas chromatograph equipped with a methanizer, thermal conductivity detector, and dual flame-

ionization detectors. A custom set of 8 columns and timed valves enable quantitative analysis of the following gases: hydrogen, nitrogen, oxygen, carbon dioxide, carbon monoxide, methane, ethane, ethylene, and ethyne. Argon serves as the carrier gas. The thermal conductivity detector (TCD) was used for quantification of H_2.

First, we conducted a single-point calibration of the GC with six replicate measurements of 79 ppm H_2 in N_2. Samples used for calibration were prepared as follows: a 3150-mL round bottom flask sealed with a rubber septum with purged with N_2 for 30 minutes, and 0.25 mL of H_2 was injected into the flask using a Vici Pressure-Lok® gas-tight syringe (see SI, Figure S35 and Table S2). For assaying generation of H_2 from trace water in MeCN, in a glovebox, 8 grams of dried CaH_2 was placed in a 250 mL round bottom flask sealed with a rubber septum, and then 20 mL of MeCN was injected into the flask and allowed to stir for 20 minutes. Using a gas-tight syringe, 10 mL of headspace was removed and promptly analyzed (see SI, Figure S37), allowing for estimation of the H_2O content of our MeCN (see SI, Tables S3 and S4).

ASSOCIATED CONTENT

Supporting Information. The following files are available free of charge.

NMR spectra of probe molecules; characterization of triflate and hexafluorophosphate salts; titration data; analysis of water content in MeCN solvent; infrared spectra (PDF)

AUTHOR INFORMATION

Corresponding Author

* To whom correspondence should be addressed. E-mail: blakemore@ku.edu. Phone: +1 (785) 864-3019.

Author Contributions

The manuscript was written through contributions of all authors. All authors have given approval to the final version of the manuscript. ‡These authors contributed equally (R.R.G. and T.D.C.)

ACKNOWLEDGMENT

The authors thank Dr. Justin Douglas and Sarah Neuenswander for assistance with NMR spectroscopy, Dr. Wade Henke for preparation of $NaBArF_{24}$, Emily Boyd for sharing insights regarding preparation of $NaBArF_{24}$, and Dr. Amit Kumar for helpful discussions regarding quantification of Lewis acidity. This work was supported by the U.S. Department of Energy, Office of Science, Office of Basic Energy Sciences through the Early Career Research Program (DE-SC0019169). C.J.P. was supported by a Clark E. Bricker Summer ChemScholar Award from the KU Department of Chemistry.

REFERENCES

[1] (a) Arnold, P. L.; Patel, D.; Wilson, C.; Love, J. B. Reduction and selective oxo group silylation of the uranyl dication. *Nature* **2008,** *451*, 315-317. (b) Buss, J. A.; VanderVelde, D. G.; Agapie, T. Lewis Acid Enhancement of Proton Induced CO_2 Cleavage: Bond Weakening and Ligand Residence Time Effects. *J. Am. Chem. Soc.* **2018,** *140*, 10121-10125. (c) Lau, T. C.; Mak, C. K. Oxidation of alkanes by barium ruthenate in acetic acid: catalysis by Lewis acids. *J. Chem. Soc., Chem. Commun.* **1993**, 766-767.

[2] (a) Kanady, J. S.; Tsui, E. Y.; Day, M. W.; Agapie, T. A Synthetic Model of the Mn3Ca Subsite of the Oxygen-Evolving Complex in Photosystem II. *Science* **2011,** *333*, 733-736. (b) Herbert, D. E.; Lionetti, D.; Rittle, J.; Agapie, T. Heterometallic Triiron-Oxo/Hydroxo Clusters: Effect of Redox-Inactive Metals. *J. Am. Chem. Soc.* **2013,** *135*, 19075-19078. (c) Tsui, E. Y.; Agapie, T. Reduction potentials of heterometallic manganese-oxido cubane complexes modulated by redox-inactive metals. *Proc. Nat. Acad. Sci. U.S.A.* **2013,** *110*, 10084-10088. (d) Kumar, A.; Lionetti, D.; Day, V. W.; Blakemore, J. D. Trivalent Lewis Acidic Cations Govern the Electronic Properties and Stability of Heterobimetallic Complexes of Nickel. *Chem. – Eur. J.* **2018,** *24*, 141-149. (e) Reath, A. H.; Ziller, J. W.; Tsay, C.; Ryan, A. J.; Yang, J. Y. Redox Potential and Electronic Structure Effects of Proximal Nonredox Active Cations in Cobalt Schiff Base Complexes. *Inorg. Chem.* **2017,** *56*, 3713-3718.

[3] Kumar, A.; Lionetti, D.; Day, V. W.; Blakemore, J. D. Redox-Inactive Metal Cations Modulate the Reduction Potential of the Uranyl Ion in Macrocyclic Complexes. *J. Am. Chem. Soc.* **2020,** *142*, 3032-3041.

[4] Perrin, D. D. *Ionisation Constants of Inorganic Acids and Bases in Aqueous Solution*. Pergamon Press: New York, 1982; pp. 180.

[5] Bang, S.; Lee, Y.-M.; Hong, S.; Cho, K.-B.; Nishida, Y.; Seo, M. S.; Sarangi, R.; Fukuzumi, S.; Nam, W. Redox-inactive metal ions modulate the reactivity and oxygen release of mononuclear non-haem iron(III)-peroxo complexes. *Nat. Chem.* **2014,** *6*, 934-940.

[6] (a) Fukuzumi, S.; Ohkubo, K. Quantitative evaluation of Lewis acidity of metal ions derived from the g values of ESR spectra of superoxide: metal ion complexes in relation to the promoting effects in electron transfer reactions. *Chem. - Eur. J.* **2000,** *6*, 4532-4535. (b) Ohkubo, K.; Suenobu, T.; Imahori, H.; Orita, A.; Otera, J.; Fukuzumi, S. Quantitative evaluation of Lewis acidity of organotin compounds and the catalytic reactivity in electron transfer. *Chem. Lett.* **2001**, 978-979.

[7] (a) Gaffen, J. R.; Bentley, J. N.; Torres, L. C.; Chu, C.; Baumgartner, T.; Caputo, C. B. A Simple and Effective Method of Determining Lewis Acidity by Using Fluorescence. *Chem* **2019,** *5*, 1567-1583. (b) Bentley, J. N.; Elgadi, S. A.; Gaffen, J. R.; Demay-Drouhard, P.; Baumgartner, T.; Caputo, C. B. Fluorescent Lewis Adducts: A Practical Guide to Relative Lewis Acidity. *Organometallics* **2020,** *39*, 3645-3655.

[8] (a) Mayer, U.; Gutmann, V.; Gerger, W. The acceptor number — A Quantitative Empirical Parameter for the Electrophilic Properties of Solvents. *Monatsh. Chem.* **1975**, *106*, 1235-1257. (b) Beckett, M. A.; Strickland, G. C.; Holland, J. R.; Sukumar Varma, K. A Convenient NMR Method for the Measurement of Lewis Acidity at Boron Centres: Correlation of Reaction Rates of Lewis Acid Initiated Epoxide Polymerizations with Lewis Acidity. *Polymer* **1996**, *37*, 4629-4631.

[9] Kumar, A.; Blakemore, J. D. On the Use of Aqueous Metal-Aqua pKa Values as a Descriptor of Lewis Acidity. *Inorg. Chem.* **2021**, *60*, 1107-1115.

[10] (a) Koito, Y.; Nakajima, K.; Kobayashi, H.; Hasegawa, R.; Kitano, M.; Hara, M. Slow Reactant-Water Exchange and High Catalytic Performance of Water-tolerant Lewis Acids. *Chem. – Eur. J.* **2014**, *20*, 8068-8075. (b) Brand, S.; Pahl, J.; Elsen, H.; Harder, S. Frustrated Lewis Pair Chemistry with Magnesium Lewis Acids. *Eur. J. Inorg. Chem.* **2017,** *2017*, 4187-4195. (c) Pahl, J.; Brand, S.; Elsen, H.; Harder, S. Highly Lewis acidic cationic alkaline earth metal complexes. *Chem. Commun.* **2018,** *54*, 8685-8688. (d) Fischer, M.; Wolff, M. C.; del Horno, E.; Schmidtmann, M.; Beckhaus, R. Synthesis, Reactivity, and Insights into the Lewis Acidity of Mononuclear Titanocene Imido Complexes Bearing Sterically Demanding Terphenyl Moieties. *Organometallics* **2020,** *39*, 3232-3239.

[11] Zheng, A.; Liu, S.-B.; Deng, F. ^{31}P NMR Chemical Shifts of Phosphorus Probes as Reliable and Practical Acidity Scales for Solid and Liquid Catalysts. *Chem. Rev.* **2017**, *117*, 12475-12531.

[12] Erdmann, P.; Greb, L. What Distinguishes the Strength and the Effect of a Lewis Acid: Analysis of the Gutmann–Beckett Method. *Angew. Chem. Int. Ed.* **2022**, *61,* e202114550.

[13] Thordarson, P. Determining Association Constants from Titration Experiments in Supramolecular Chemistry. *Chem. Soc. Rev.* **2011**, *40*, 1305-1323.

[14] (a) Hill, A. V. The Possible Effects of the Aggregation of the Molecules of Haemoglobin on its Dissociation Curves. *J. Physiol.* **1910**, *40*, 4-7. (b) Langmuir, I. The Adsorption of Gases on Plane Surfaces of Glass, Mica and Platinum. *J. Am. Chem. Soc.* **1918**, *40*, 1361-1403. (c) Berg, J. M.; Tymoczko, J. L.; Stryer, L. *Biochemistry*; Macmillan, **2007**, 210-211.

[15] Berthet, J.-C.; Nierlich, M.; Ephritikhine, M. Uranium Triflate Complexes. *C. R. Chim.* **2002**, *5*, 81-87.

[16] Berthet, Jean C.; Lance, M.; Nierlich, M.; Ephritikhine, M. Simple Preparations of the Anhydrous and Solvent-Free Uranyl and Cerium(IV) Triflates $UO_2(OTf)_2$ and $Ce(OTf)_4$ − Crystal Structures of $UO_2(OTf)_2(py)_3$ and $[\{UO_2(py)_4\}2(\mu\text{-}O)][OTf]_2$. *Eur. J. Inorg. Chem.* **2000**, *2000*, 1969-1973.

[17] (a) Harris, R. K.; Becker, E. D.; Cabral de Menezes, S. M.; Goodfellow, R.; Granger, P. NMR nomenclature. Nuclear Spin Properties and Conventions for Chemical Shifts (IUPAC Recommendations 2001). *Pure Appl. Chem.* **2001**, *73*, 1795-1818. (b) Harris, R. K.; Becker, E. D.; Cabral De Menezes, S. M.; Granger, P.; Hoffman, R. E.; Zilm, K. W. Further Conventions for NMR Shielding and Chemical Shifts: (IUPAC Recommendations 2008). *Pure Appl. Chem.* **2008,** 80, 59-84.

[18] (a) Widdifield, C. M.; Schurko, R. W. Understanding Chemical Shielding Tensors using Group Theory, MO analysis, and Modern Density-functional Theory. *Concepts in Magn. Reson. A* **2009**, *34A*, 91-123. (b) Un, S.; Klein, M. P. Study of Phosphorus-31 NMR Chemical Shift Tensors and their Correlation to Molecular Structure. *J. Am. Chem. Soc.* **1989**, *111*, 5119-5124.

[19] Shannon, R. D. Revised Effective Ionic Radii and Systematic Studies of Interatomic Distances in Halides and Chalcogenides. *Acta Cryst. A* **1976**, *32*, 751-767.

[20] (a) Neilson, G. W.; Skipper, N. K+ coordination in aqueous solution. *Chem. Phys. Lett.* **1985,** *114*, 35-38. (b) Soper, A. K.; Weckström, K. Ion solvation and water structure in

potassium halide aqueous solutions. *Biophys. Chem.* **2006,** *124*, 180-191. (c) Glezakou, V.-A.; Chen, Y.; Fulton, J. L.; Schenter, G. K.; Dang, L. X. Electronic structure, statistical mechanical simulations, and EXAFS spectroscopy of aqueous potassium. *Theor. Chem. Acc.* **2006,** *115*, 86-99. (d) Rowley, C. N.; Roux, B. t. The Solvation Structure of Na^+ and K^+ in Liquid Water Determined from High Level ab Initio Molecular Dynamics Simulations. *J. Chem. Theor. Comp.* **2012,** *8*, 3526-3535.

[21] Jennings, J. J.; Wigman, B. W.; Armstrong, B. M.; Franz, A. K. NMR Quantification of the Effects of Ligands and Counterions on Lewis Acid Catalysis. *J. Org. Chem.* **2019**, *84*, 15845-15853.

[22] (a) Reger, D. L.; Little, C. A.; Lamba, J. J. S.; Brown, K. J.; Krumper, J. R.; Bergman, R. G.; Irwin, M.; Fackler, J. P., Jr. Main Group Compounds. Sodium tetrakis(3,5-bis(trifluoromethyl)phenyl)borate, $Na[B(3,5\text{-}(CF_3)_2C_6H_3)_4]$. *Inorg. Synth.* **2004**, *34*, 5-8. (b) Park, J. G.; Jeon, I.-R.; Harris, T. D. Electronic Effects of Ligand Substitution on Spin Crossover in a Series of Diiminoquinonoid-Bridged Fe^{II}_2 Complexes. *Inorg. Chem.* **2015**, *54*, 359-369. (c) Boelke, A.; Kuczmera, T. J.; Lork, E.; Nachtsheim, B. J. N-Heterocyclic Iodazolium Salts – Potent Halogen-Bond Donors in Organocatalysis. *Chem. – Eur. J.* **2021**, *27*, 13128-13134.

[23] Takaoka, A.; Gerber, L. C. H.; Peters, J. C. Access to Well-Defined Ruthenium(I) and Osmium(I) Metalloradicals. *Angew. Chem. Int. Ed.* **2010**, *49*, 4088-4091.

[24] (a) Xu, K. Nonaqueous Liquid Electrolytes for Lithium-Based Rechargeable Batteries. *Chem. Rev.* **2004,** *104*, 4303-4418. (b) Aravindan, V.; Gnanaraj, J.; Madhavi, S.; Liu, H.-K. Lithium-Ion Conducting Electrolyte Salts for Lithium Batteries. *Chem. – Eur. J.* **2011,** *17*, 14326-14346.

[25] (a) Barlowz, C. G. Reaction of Water with Hexafluorophosphates and with Li Bis(perfluoroethylsulfonyl)imide Salt. *Electrochem. Solid-State Lett.* **1999,** *2*, 362-364. (b) Stich, M.; Göttlinger, M.; Kurniawan, M.; Schmidt, U.; Bund, A. Hydrolysis of $LiPF_6$ in Carbonate-Based Electrolytes for Lithium-Ion Batteries and in Aqueous Media. *J. Phys. Chem. C* **2018,** *122*, 8836-8842.

[26] (a) Kock, L. D.; Lekgoathi, M.; Crouse, P. L.; Vilakazi, B. Solid State Vibrational Spectroscopy of Anhydrous Lithium Hexafluorophosphate ($LiPF_6$). *J. Mol. Struct.* **2012**, *1026*, 145-149. (b) Lekgoathi, M. D. S.; Vilakazi, B. M.; Wagener, J. B.; Le Roux, J. P.; Moolman, D. Decomposition Kinetics of Anhydrous and Moisture Exposed $LiPF_6$ Salts by Thermogravimetry. *J. Fluor. Chem.* **2013**, *149*, 53-56.

[27] (a) Mathur, J. N.; Murali, M. S.; Nash, K. L. Actinide Partitioning–A Review. *Solvent Extraction and Ion Exchange* **2001,** *19*, 357-390. (b) Khopkar, P. K.; Mathur, J. N. Synergistic Extraction of Trivalent Actinides by Mixtures of Thenoyltrifluoroacetone and Neutral Oxo Donors. *Sep. Sci. Technol.* **1981**, *16*, 957-969.

[28] Groom, C. R.; Bruno, I. J.; Lightfoot, M. P.; Ward, S. C. The Cambridge Structural Database. *Acta Cryst. B* **2016,** *72*, 171-179.

[29] Moaven, S.; Unruh, D. K.; Cozzolino, A.F.; CCDC 1822195: Experimental Crystal Structure Determination, **2018**, doi: 10.5517/ccdc.csd.cc1z54hs.

[30] (a) Crisp, M.G.; Rendina, L.M.; Tiekink, E.R.T.; CCDC 170427: Experimental Crystal Structure Determination, **2001**, doi: 10.5517/cc5qbnv (b) Crisp, M.G.; Rendina, L.M.; Tiekink, E.R.T., Crystal structure of trans-bis(diethylhydroxyphosphine)

diethylphosphinito(iodo)platinum(II) triethylphosphineoxide solvate (1/1),[$(Et_2(OH)P)_2(Et_2PO)IPt] \cdot Et_3PO$. *Z. Kristallogr.* **2001,** *216*, 243-244.[

[31] (a) Polezhaev, A. V.; Maciulis, N. A.; Chen, C.; Pink, M.; Lord, R. L.; Caulton, K. G., CCDC 1971824: Experimental Crystal Structure Determination, **2019**, doi: 10.5517/ccdc.csd.cc245v7f. (b) Polezhaev, A. V.; Maciulis, N. A.; Chen, C.-H.; Pink, M.; Lord, R. L.; Caulton, K. G., Tetrazine Assists Reduction of Water by Phosphines: Application in the Mitsunobu Reaction. *Chem. Eur. J.* **2016,** *22*, 13985-13998.

[32] (a) Doan-Nguyen, V.V.T.; Carrol, P.J.; Murray, C.B.; CCDC 1048929: Experimental Crystal Structure Determination, **2015**, doi: 10.5517/cc146hf8. (b) Doan-Nguyen, V.V.T.; Carrol, P.J.; Murray, C.B. Structure determination and modeling of monoclinic trioctylphosphine oxide. *Acta Cryst. C* **2015**, *71*, 239-241.

[33] (a) Baures, P.W; Silverton, J.V.; CCDC 1183966: Experimental Crystal Structure Determination, **1990**, database identifier: JEDTOB. (b) Baures, P.W; Silverton, J.V.; Structure of triphenylphosphine oxide hemihydrate. *Acta Cryst. C* **1990**, *46*, 715-717.

[34] (a) Baures, P.W; CCDC 1183967: Experimental Crystal Structure Determination, **1992**, database identifier: JEDTOB01. (b) Baures, P.W; Monoclinic triphenylphosphine oxide hemihydrate. *Acta Cryst. C* **1991**, *47*, 2715-2716.

[35] (a) Ng, S.W. CCDC 738316: Experimental Crystal Structure Determination, **2009**, doi: 10.5517/ccss8ng. (b) Ng, S.W. A Second Monoclinic Modification of Triphenylphosphine Oxide Hemihydrate. *Acta Cryst. E* **2009**, *65*, o1431.

[36] The values for the average P–O distances were calculated as the arithmetic mean of the values in the available structures. The stated e.s.d.'s on these distances are taken as the largest of the original e.s.d. values in the refined data for the independent structures.

[37] Dahlquist, F. W. The Meaning of Scatchard and Hill Plots. *Methods Enzymol.* **1978**, *48*, 270-299.

[38] Fulmer, G. R.; Miller, A. J. M.; Sherden, N. H.; Gottlieb, H. E.; Nudelman, A.; Stoltz, B. M.; Bercaw, J. E.; Goldberg, K. I. NMR Chemical Shifts of Trace Impurities: Common Laboratory Solvents, Organics, and Gases in Deuterated Solvents Relevant to the Organometallic Chemist. *Organometallics* **2010**, *29*, 2176-2179.

TOC Graphic

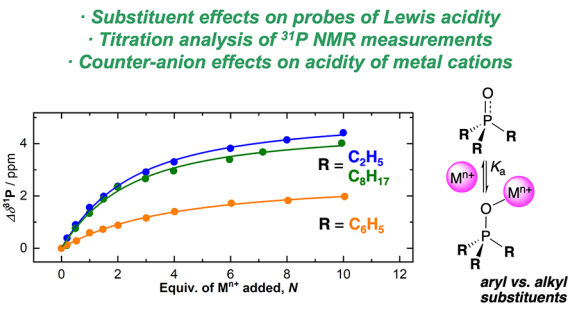

TOC Synopsis

New ^{31}P NMR measurements have been used to investigate how the structure of phosphine oxides affects their usefulness for quantification of the Lewis acidity of metal cations. Using titration data, the binding affinity of different probes for the metal cations have been compared, as well as their overall speciation in the presence of variable concentrations of metal cations. The findings show that trialkylphosphine oxides display intrinsically wider dynamic ranges than triphenylphosphine oxide.